Global Biogeochemical Cycles

RESEARCH ARTICLE
10.1029/2025GB008560

Composition and Plume Gas Interaction Control Iron Fractional Solubility More Than Particle Size in Volcanic Ash: Implications for Fertilization of the North Atlantic

H. E. Elliott[1,2], E. Blades[3], H. M. Royer[4,5], C. Buck[6], C. Kollman[6], R. Kukkadapu[7], S. China[7], Z. Cheng[7], N. N. Lata[7], M. Engelhard[7], M. Bowden[7], N. Lahiri[7], R. L. Parham[8], L. Meagher[8], B. Angstman[8], A. P. Ault[8], A. Hornby[9,10], K. Dayton[9], E. Gazel[9], and C. J. Gaston[4]

[1]Department of Ocean Sciences, Rosenstiel School of Marine, Atmospheric and Earth Science, University of Miami, Miami, FL, USA, [2]Now at Department of Biological & Environmental Sciences, Wittenberg University, Springfield, OH, USA, [3]Barbados Atmospheric Chemistry Observatory, Ragged Point, Barbados, [4]Department of Atmospheric Sciences, Rosenstiel School of Marine, Atmospheric and Earth Science, University of Miami, Miami, FL, USA, [5]Now at Department of Environmental Sciences and Engineering, Gillings School of Public Health, University of North Carolina—Chapel Hill, Chapel Hill, NC, USA, [6]Department of Marine Sciences, Skidaway Institute of Oceanography, University of Georgia, Savannah, GA, USA, [7]Pacific Northwest National Laboratory, Richland, WA, USA, [8]Department of Chemistry, University of Michigan, Ann Arbor, MI, USA, [9]Department of Earth and Atmospheric Sciences, Cornell University, Ithaca, NY, USA, [10]Now at Center for Biomedical Research, Health Science Center, University of Texas at Tyler, Tyler, TX, USA

Key Points:

- All volcanic ash samples analyzed have fractional iron solubilities of <6%, but solubility varies
- Differences in iron fractional solubility for ash can be explained primarily by ash particle composition and plume processing

Supporting Information:

Supporting Information may be found in the online version of this article.

Correspondence to:

C. J. Gaston,
cgaston@miami.edu

Citation:

Elliott, H. E., Blades, E., Royer, H. M., Buck, C., Kollman, C., Kukkadapu, R., et al. (2025). Composition and plume gas interaction control iron fractional solubility more than particle size in volcanic ash: Implications for fertilization of the North Atlantic. *Global Biogeochemical Cycles*, *39*, e2025GB008560. https://doi.org/10.1029/2025GB008560

Received 3 MAR 2025
Accepted 13 AUG 2025

Author Contributions:

Conceptualization: H. E. Elliott, E. Blades
Formal analysis: H. M. Royer, C. Kollman, R. Kukkadapu, Z. Cheng, N. N. Lata, M. Engelhard, M. Bowden, N. Lahiri, R. L. Parham, L. Meagher, B. Angstman, A. Hornby
Funding acquisition: A. P. Ault
Investigation: H. E. Elliott, C. Kollman, R. Kukkadapu
Methodology: H. E. Elliott, H. M. Royer, C. Buck, C. Kollman, R. Kukkadapu, Z. Cheng, R. L. Parham, A. P. Ault, A. Hornby
Resources: E. Blades, C. Buck, S. China, A. P. Ault, K. Dayton, E. Gazel

Abstract Deposition of volcanic ash is thought to impact marine biogeochemical cycling by adding soluble iron (Fe) to the surface ocean. The magnitude of this input is a function of the amount of ash deposited, the total Fe content in the ash, and ash-derived Fe's fractional solubility. However, the relative importance of chemical composition, acidic processing by the volcanic plume, and ash particle size in determining solubility is unclear. We paired an aerosol leach meant to provide an upper limit for fractional Fe solubility with chemical analyses of ash from the Cumbre Vieja (CV) and La Soufrière eruptions, which both impacted the North Atlantic in 2021. Fe in the ash samples is <6% soluble, but Fe fractional solubility in CV ash is approximately triple that of La Soufrière ash. Compared to La Soufrière, a larger proportion of the Fe in CV ash is in silicate rather than oxide minerals, which release more soluble Fe. Elevated levels of surficial fluorine (F) also suggest that CV ash was subjected to a more fluorine-rich eruption plume and underwent more acidic processing. Particle size does not appear to be a primary control on Fe release. We estimate that the CV eruption had a much larger impact on dissolved Fe (DFe) concentration in the surface ocean than the La Soufrière eruption because of differences in soluble Fe content and particle deposition velocity. These differences may help explain why some eruptions elicit a biological response in the ocean while others do not.

Plain Language Summary Volcanic ash deposition into the surface ocean supplies seawater with iron (Fe), an important nutrient for marine microbial life. However, we analyzed ash from two recent eruptions and found that <6% of the total Fe in the ash is soluble and potentially available for microbial uptake. Our results suggest that Fe in ash is less soluble than Fe in mineral dust, a major aerosol input to the North Atlantic Ocean. We found that particle composition and processing by the volcanic plume, rather than ash particle size, are the dominant controls on soluble Fe release from volcanic ash. We conclude that some, but not all, eruptions likely add enough soluble Fe to the surface ocean to fuel marine biota.

1. Introduction

Fertilization of marine ecosystems through deposition of volcanic material has been proposed as a catalyst for a variety of atmospheric carbon dioxide (CO_2)-drawdown events that span geologic history. These include major climatic shifts like the cooling periods after the Paleocene/Eocene thermal maximum (PETM; ~55 Mya) and at the Eocene-Oligocene boundary (~34 Mya) (Bains et al., 2000; Bay et al., 2004; Jicha et al., 2009), the 1991 "Pinatubo carbon anomaly" (Sarmiento, 1993), and an array of recent localized phytoplankton blooms (Hamme et al., 2010; Langmann et al., 2010; Vergara-Jara et al., 2021). Many studies suggest that volcanic material stimulates phytoplankton growth and promotes CO_2 drawdown by specifically relieving iron (Fe) limitation (Bay

Visualization: H. E. Elliott, C. Kollman, R. L. Parham, B. Angstman, A. P. Ault
Writing – original draft: H. E. Elliott, H. M. Royer
Writing – review & editing: H. E. Elliott, C. Buck, R. Kukkadapu, S. China, Z. Cheng, N. N. Lata, M. Engelhard, M. Bowden, N. Lahiri, R. L. Parham, L. Meagher, B. Angstman, A. P. Ault, A. Hornby

et al., 2004; Langmann et al., 2010; Sarmiento, 1993; Spirakis, 1991), with Duggen et al. (2010) even proposing that volcanic-derived Fe inputs to the surface ocean may be nearly as important as Fe inputs from aeolian dust.

Fe fertilization from volcanic ash is theoretically possible. Volcanic ash often contains more bulk Fe content than mineral dust (Elliott et al., 2024; Geisen et al., 2022) due to the presence of Fe-rich minerals, including salts, that coat ash particles (Duggen et al., 2010; Langmann et al., 2010). Upon deposition in seawater, these salt coatings are thought to dissolve readily enough to have biological significance in the surface ocean (Duggen et al., 2010; Jones & Gislason, 2008; Langmann et al., 2010). Additionally, strong acids (e.g., sulfuric, hydrochloric, and hydrofluoric) in volcanic plumes can solubilize Fe (Duggen et al., 2010; Hoshyaripour et al., 2015; Maters et al., 2017; Oakes et al., 2012), and photochemical reactions and interactions with co-emitted sulfur likely reduce Fe(III) in ash to Fe(II), increasing its solubility (Bay et al., 2004; Hoshyaripour et al., 2014; Wadsworth et al., 2021).

Despite this potential for soluble Fe release, verifying that Fe fertilization supports post-eruption phytoplankton blooms observed after volcanic eruptions has proven challenging. Many studies on volcanic ash deposition into seawater are satellite-based, but ash particles in the air and surface ocean can interfere with satellite-derived chlorophyll-*a* (Chl-α) and phytoplankton abundance estimates (Bisson et al., 2023; Browning et al., 2015; Claustre et al., 2002). Limited laboratory and mesocosm studies have demonstrated both increased and decreased growth rates of marine microbial species (Hoffmann et al., 2012) and shifts in microbial community composition (Zhang et al., 2017) after volcanic ash addition.

While some attempts at standardization of ash collection and leaching protocols have been made (Gislason et al., 2011; Perron et al., 2020; Stewart et al., 2013, 2020; Witham et al., 2005), to date, many existing laboratory measurements of soluble Fe are complicated by the use of different leaching techniques and solvents with a range of ionic strengths and pH values (i.e., deionized water, seawater, or acidic solutions; Duggen et al., 2010). These differences in methodology make it difficult to compare Fe solubility estimates between different types of volcanic material or with those for other aerosol types (Meskhidze et al., 2019).

Even when studies use identical leaching methodologies, samples from different volcanic eruptions are too chemically different for a single global estimate to be meaningful for implementation in a deposition model. Jones and Gislason (2008), for example, documented the dissolution of 0.02–7.09 μmol Fe/g ash into Atlantic surface seawater in flow-through reactors over 8 hr for ash from just four different eruptions. Olgun et al. (2011) leached 44 volcanic ash samples from 16 different volcanoes into buffered (pH = 8), filtered (0.2 μm) Atlantic seawater supplemented with an organic ligand (a thiazolyazo compound) and documented dissolution of 0.035–0.340 μmol Fe/g ash during a 60-min leach. Olgun et al. (2011) reported bulk Fe fractional solubilities for ash that range over tenfold (<0.01%–0.1%) in seawater. Overall, leaching studies have suggested that Fe fractional solubility for volcanic ash is generally in the range suggested by Olgun et al. (2011) but can be as high as ∼1% (Ayris & Delmelle, 2012; Duggen et al., 2010). The models designed to estimate Fe deposition often ignore volcanic emissions as a source of soluble Fe (Myriokefalitakis et al., 2018). More measurements of soluble Fe content in volcanic ash are necessary to improve model estimates (Myriokefalitakis et al., 2018).

The differences in soluble Fe content between different types of volcanic material likely result from differences in plume composition, the amount of processing ash is subjected to within the volcanic plume, ash particle composition, and ash particle size. Baker and Jickells (2006) used an ammonium acetate (pH = 4.7) leach to measure soluble Fe in aerosols collected over the Atlantic Ocean. They concluded that surface area-to-volume ratio, and therefore particle size, is the main factor controlling Fe solubility in mineral aerosols (Baker & Jickells, 2006). Conversely, Buck et al. (2010) found no clear relationship between aerosol Fe solubility and particle size for aerosol collected over the North Atlantic using a deionized water (pH = 5.6) leach. Journet et al. (2008) leached crushed minerals in nitric acid (pH = 2) and found that Fe solubility tends to be low in Fe (hydr-)oxide minerals like magnetite, goethite, and hematite despite their high total Fe content because Fe is tied up in strong covalent bonds. Fe solubility tends to be higher when Fe is held with ionic bonds or found as impurities (Journet et al., 2008). Which of the aforelisted factors is the dominant control on soluble Fe release in volcanic ash, and aerosols in general, remains unclear. Filling this knowledge gap would allow for a better understanding of aerosols' potential to fertilize the ocean.

To better understand the factors that influence Fe solubility in volcanic ash, a standardized aerosol leaching procedure must be coupled with chemical and single-particle techniques that enable us to examine particle composition, Fe mineralogy, and particle size. For analysis of fractional Fe solubility, we used a leach developed by

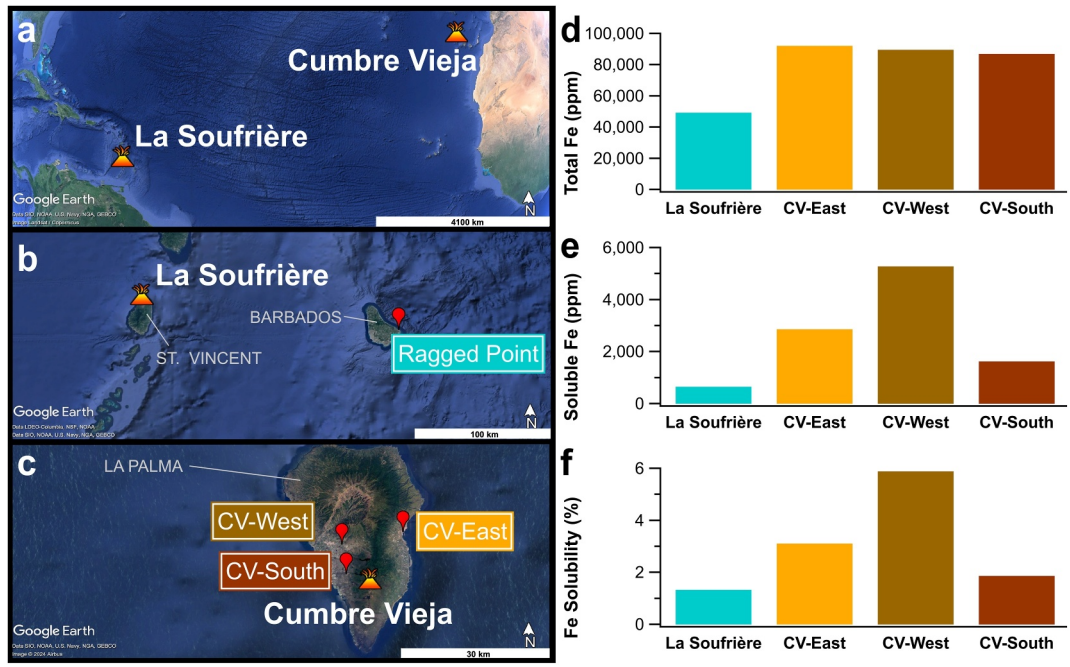

Figure 1. Locations of the La Soufrière and Cumbre Vieja (CV) eruptions (a), location of Ragged Point, Barbados, in relation to the La Soufrière eruption (b), and collection locations for the CV samples on La Palma (c) are displayed on the left. Total Fe (d), soluble Fe (e), and percent Fe solubility (f) for ash from both eruptions are shown on the right. Error on total and soluble Fe measurements is reported as % RSDs in Table S1 in Supporting Information S1 (% RSDs were <7% for both total and soluble Fe measurements on the ICP-MS).

Berger et al. (2008) that involves the use of a weak acid combined with a reducing agent and a short heating step. This leach provides a measurement of the "upper limit" for fractional Fe solubility by extracting labile forms of aerosol Fe potentially bioavailable to marine microbes without releasing refractory Fe within minerals that can be released with more rigorous leaches (Baker & Croot, 2010; Berger et al., 2008; Shelley et al., 2018). In this study, volcanic ash collected from two eruptions in 2021 provided an opportunity to study the mechanisms of Fe solubility in volcanic material and compare ash's soluble Fe to that of mineral dust collected in a region that receives high dust loads annually. La Soufrière (alternatively Soufrière St. Vincent) is a volcano located on St. Vincent in the Caribbean that was largely inactive for over 40 years until over 30 eruptive events occurred from April 9-22, 2021, releasing plumes of ash and gas (Joseph et al., 2022; Ravindra Babu et al., 2022; Taylor et al., 2023; Figure 1). The Cumbre Vieja (CV) volcanic ridge (Tajogaite volcano) is located on the eastern side of the Atlantic basin on La Palma in the Canary Islands (Caballero et al., 2022; Figure 1). Also inactive since the 1970s, it erupted from 19 September–13 December 2021, with both lava flows to the ocean and airborne injection of ash (Caballero et al., 2022; De Luca et al., 2022; Milford et al., 2023). While the eruptions, their magma composition, and ash particle properties were very different, both occurred on islands in the North Atlantic Ocean in a similar volcanic setting (Text S1 in Supporting Information S1). Analysis of both types of ash can therefore serve as a case study on variability in aerosol Fe fractional solubility for volcanic materials regularly impacting the surface ocean.

2. Materials and Methods

2.1. Sample Collection

La Soufrière ash samples were collected at Ragged Point, Barbados (13°6′N, 59°37′W; <200 km from La Soufrière) in April 2021 (Text S2 in Supporting Information S1). The sample used for soluble Fe analysis was collected atop a Whatman 41 filter using a high-volume aerosol sampler on a 17-m collection tower and shielded from rain exposure. Three ash samples from the CV eruption were collected from different locations on La Palma post-deposition in October 2021 (Figure 1; Figures S1–S3 in Supporting Information S1). These three samples are called CV-East, West, and South throughout the text based on collection location. The CV-East sample was

collected at 28°40.800′N, 17°46.077′W and, notably, was exposed to a light rain prior to collection. The CV-West sample was collected at 28°39.369′ N, 17° 53.420′W. The CV-South sample was collected at 28°36.067′N, 17°52.934′W (collection of each sample is described in Text S2 in Supporting Information S1). More well-studied aerosol samples were also collected to use as a basis of comparison with the Fe solubility leach: two volcanic ash samples from the 2010 Eyjafjallajökull eruption were collected at Stórhöfði, Iceland (63°23.885′N 20°17.299′W, 118 m asl atop a Whatman 41 filter using a high-volume sampler; see Prospero et al., 2012) on 14–15 May 2010, and two mineral dust samples were collected on Whatman 41 cellulose filters at Ragged Point, Barbados in June 2020 (18–19 and 26–27 June) (Elliott et al., 2024). While the particle size cutoff for collection on Whatman 41 filters is at least 80–100 μm in diameter due to the geometry of the rainhat (Barkley et al., 2021; Royer et al., 2023), it should be noted that the La Soufrière and Eyjafjallajökull samples collected "atop" Whatman 41s were poured off of filters saturated with material, so the collection method was not dissimilar to that used for the CV ash.

2.2. Fe Solubility (Berger) Leach

We measured the soluble Fe content using a leach that combines a weak acid with a reducing agent and a short heating step (Berger et al., 2008). This leach is meant to release surficial labile trace metals, for example, iron oxyhydroxide coatings, and the potentially bioavailable fraction of the particulate pool without releasing the refractory portion within minerals (Berger et al., 2008; Text S3 in Supporting Information S1). The Berger et al. (2008) leach has been used to define an "upper limit" for Fe solubility in aerosol samples and to estimate the fraction of Fe that is potentially bioavailable to marine microbes during aerosols' residence time in the ocean's euphotic zone (Shelley et al., 2018). This method does not consider processes that occur after deposition to seawater, such as organic complexation, photochemistry, and scavenging (Baker & Croot, 2010; Shelley et al., 2018). 10–70 mg of volcanic material was folded into ∼26 cm^2 of Whatman-41 (W-41) cellulose filter paper, which was placed in a centrifuge tube. Following the procedure from Berger et al. (Berger et al., 2008; see Text S3 in Supporting Information S1 for details), 5 mL of a 25% (v/v) acetic acid and 0.02 M hydroxylamine hydrochloride solution (pH = 2) was added to each tube, and the sample tubes were submerged in a hot water bath (90–95°C) for 10 min. The samples were removed from heat, uncapped under a laminar flow hood in a clean room environment, and left to cool for 110 min. After 2 hours of total leaching time, the tubes were capped and centrifuged at 4,500 rpm for 5 minutes, then the liquid was decanted into acid-cleaned perfluoro alkoxy (PFA) vials under a laminar flow hood. In two sequential steps, 2.5 mL of ultrapure (≥18.2 MΩ·cm; UHP) water was added to each vial, centrifuged again and decanted to the PFA vial. The decanted solutions were acidified with 100 μL of double-distilled concentrated HNO_3. The leach solutions were evaporated to near dryness and then redissolved in 2% (v/v) Optima HNO_3. This same process was completed without sample material to assess the procedural blank. Samples were diluted with 2% Optima HNO_3 as necessary and Fe concentrations in the leachate were measured with a Perkin Elmer NexION 300D inductively coupled mass spectrometer (ICP-MS; Text S4 in Supporting Information S1). As a basis for comparison, the Fe solubility leach was also performed using the ash samples from the 2010 Eyjafjallajökull eruption and mineral dust samples from June 2020. For the mineral dust samples on filter paper, 1/16 of a filter was used in the leach (<10 mg aerosol). Aerosol mass on filters was determined by ashing filter portions at 500°C to remove the cellulose filter component and weighing the remaining ash (Elliott et al., 2024).

2.3. Total Fe Measurement

To determine total Fe content in the samples, 15–85 mg of sample was digested in 10 mL of a tri-acid cocktail (1 distilled HNO_3: 2 distilled HCl: 1 distilled HF) at 150°C, evaporated to dryness, and resuspended in 6M HNO_3. Volcanic ash samples from the 2010 Eyjafjallajökull eruption and mineral dust samples were also analyzed for comparison. Prior to digestion, the filters with mineral dust were ashed at 500°C to remove the cellulose filter (Text S5 in Supporting Information S1). Samples redissolved in 6M HNO_3 were diluted 30× in milliQ water, further diluted with 2% HNO_3 as necessary, and then analyzed for total Fe using a NexION 300D system (see Table S3 in Supporting Information S1 for %RSDs on measurements for soluble and total Fe).

2.4. Microscopy

Particles of both the La Soufrière and La Palma samples were mounted on carbon adhesive (PELCO Carbon Conductive tabs) and analyzed using Scanning Electron Microscopy (SEM) coupled with Energy Dispersive Spectroscopy (EDX, EDAX Genesis detector). The SEM was equipped with an FEI Quanta digital field emission gun (operated at 20 kV accelerating voltage and 480 pA current). The SEM chamber is 293 K under vacuum

conditions ($\sim 1.2 \times 10^{-6}$ Torr pressure), where volatile and semivolatile materials might evaporate. Elemental mapping of particles, which shows the relative abundance of select elements spatially throughout individual particles (Ault et al., 2012), was performed using an Oxford Instrument detector and AZtec software.

2.5. X-Ray Fluorescence (XRF) and X-Ray Photoelectron Spectroscopy (XPS)

To determine the bulk elemental composition, μ-XRF analysis was performed on a Bruker Tornado M4 Plus instrument operating at a chamber pressure of 2 mbar (Text S6 in Supporting Information S1). Surface atomic percent composition was determined through X-Ray Photoelectron Spectroscopy (XPS). This was achieved utilizing a Physical Electronics Quantera Scanning X-ray Microprobe (Text S7 in Supporting Information S1).

2.6. Mössbauer Spectroscopy

Mössbauer spectra were collected at multiple temperatures to characterize and quantify Fe-species present in the La Soufrière and CV-West samples (CV-West is the CV sample with the highest Fe fractional solubility.). CV-South, the sample from this eruption with the lowest Fe fractional solubility, was also analyzed at room temperature (RT) to confirm that the CV-West sample's Mössbauer spectrum is representative of the CV samples as a whole. Since the spectra for the two samples were very similar, only the CV-West data are modeled and discussed here. Spectra were collected using a 75 mCi (initial strength) 57Co/Rh source. The velocity transducer (WissEl Elektronik, Germany) was operated in a constant acceleration mode (23 Hz, ±12 mm/s). An Ar-Kr proportional counter was used to detect the radiation transmitted through the holder, and the counts were stored as a function of energy (transducer velocity, 1,024 channels). Raw data were folded into 512 channels to give a flat background and a zero-velocity position corresponding to the center shift of a metal iron foil at 298 K (RT). Calibration spectra were obtained with a 7 μm thick α-Fe(m) foil (Amersham, England). A closed-cycle cryostat (SHI-850, Janis Research Company, Inc., Wilmington, MA) coupled with a Sumitomo CKW He compressor unit (Allentown, Pennsylvania) was used to decrease the temperature from RT to the desired below RT temperature. Recoil software (University of Ottawa, Canada) was used for folding and modeling the data, which were modeled using the Voight-based method (Rancourt & Ping, 1991). For modeling, the Lorentzian half-width at maximum of doublet and sextet was fixed at 0.156 mm/s. For tabulating the relative percent of various Fe species, the recoilless free fractions of all the species were considered equal. A Rigaku SmartLab SE Bragg-Brentano diffractometer equipped with a Cu anode operated at 44 kV and 40 mA and a D/teX Ultra 250 1D detector was used to confirm mineral identification from the Mössbauer analysis (Text S8 in Supporting Information S1).

2.7. Particle Size Measurements

Particle size was analyzed using a Coulter Counter rather than laser diffraction because of the Coulter Counter's ability to more accurately size polydisperse samples and samples with multiple particle types. Ash samples suspended in ISOTON II electrolyte were analyzed using a Multisizer 4e Coulter Counter (Beckman Coulter) to obtain the size distribution data based on the particles' volumetric equivalent diameters (dve). Unfiltered ash samples were analyzed using a 200 μm aperture (accurate for the 4–120 μm size range) for preliminary estimates of particle abundance in the size range up to 120 μm (Text S9 and Figure S4 in Supporting Information S1). For more accurate size estimates in the smaller size ranges relevant to oceanic deposition, ash samples were pre-filtered (Text S9 in Supporting Information S1) and then analyzed using smaller apertures. Samples were analyzed using a 100 μm aperture (accurate for the 2.4–59.8 μm size range) and a 30 μm aperture (accurate for the 0.69–17.9 μm size range; see SI for information on instrument calibration). 400 size bins were used for all Coulter Counter analyses. Each blank and sample was analyzed in triplicate, with 1,000 μL analyzed per run with the 200 μm aperture and 500 μL analyzed per run with the 100 and 30 μm apertures, and counts were averaged from the three runs (Figure S2 in Supporting Information S1). Mode particle size was determined for the CV-East and CV-South samples based on Coulter Counter analysis. Lognormal fits for the size data were produced using IGOR Pro 9.05's built-in curve fitting option, and the mode size for each sample was estimated from its LogNormal fit.

The mode of the particle size distribution was submicron for La Soufrière and CV-West and was too small to be accurately determined using the Coulter Counter with the 30-μm aperture. Nanoparticle Tracking Analysis (NTA) was therefore used for sizing submicron particles (size range from 1 to 973.9 nm) from a separate sample of ash collected in Barbados after the La Soufrière eruption with a similar size distribution. This sizing method has been

used in the past for aerosol particle analysis (Axson et al., 2015; Creamean et al., 2016) and is described in detail in the Text S10 in Supporting Information S1.

The Coulter Counter is known for being able to determine the size of aspherical particles well, as long as the particles are not too porous or plate-like, as it directly measures particle volume (Allen, 2003). The NTA may be more affected by non-spherical particles, but there is evidence that it can measure the size of rod-like particles (Hoover & Murphy, 2020). Future studies would be required to determine a more direct size comparison between these (and other) methods, such as projected area diameter from SEM.

3. Results

3.1. Total and Soluble Fe Content

The three volcanic ash samples from the CV eruption have similar total Fe content, with an average of 9.0% ± 0.3% Fe by weight (error on averages represents variation among different samples from the eruption), which is roughly double that of the La Soufrière ash (4.9%; Figure 1).

Our soluble Fe leaching methodology (Berger et al., 2008) provides an upper-limit for Fe solubility and has been adopted for use in Fe bioavailability studies in the oceanographic community (Chester & Hughes, 1967; Perron et al., 2020; Shelley et al., 2018). La Soufrière ash also has the lowest soluble Fe content (6.6×10^2 ppm). The soluble Fe content for the CV samples is much more variable than the total Fe content in ash from that eruption, with CV-West having 5.3×10^3 ppm soluble Fe, approximately eight-fold that of the La Soufrière sample, followed by CV-East (2.9×10^3 ppm soluble Fe), and CV-South (1.6×10^3 ppm soluble Fe). We, therefore, estimate that Fe in ash from the La Soufrière eruption is about 1.3% soluble, while Fe in ash from the CV eruption ranges from 1.9% to 5.9% soluble. As a comparison, we measured the average total Fe content (5.4% ± 0.7%), soluble Fe content ($1.1 \times 10^3 \pm 7.8 \times 10^2$ ppm), and Fe solubility (2.1% ± 1.7%) in volcanic ash from the Eyjafjallajökull eruption in Iceland in 2010, which are all between the averages for ash from the La Soufrière and CV eruptions. Mineral dust collected at Barbados after being transported across the North Atlantic during the "Godzilla" dust event (Elliott et al., 2024) contains 4.1% ± 0.3% total Fe, with $3.8 \times 10^3 \pm 8.4 \times 10^2$ ppm soluble Fe, resulting in an average Fe solubility of 9.3% ± 1.4%.

3.2. Chemical Composition of Ash Particles

X-Ray Fluorescence (XRF) and SEM were used to further analyze the bulk and single-particle elemental composition of the ash, respectively, while XPS was used to analyze the surficial composition. Large amounts of silicon (Si) and aluminum (Al) in all ash samples indicate the presence of volcanic glass and aluminosilicate minerals (Hornby et al., 2023; Figure 2). Compared to the La Soufrière sample, XRF analysis confirmed that the CV samples are more mafic with higher levels of Fe and magnesium (Mg) (Table S2 in Supporting Information S1). The SEM images show that particles from the CV eruption vary immensely in size and morphology, with many exhibiting a glassy or porous texture (Figure 2). Relatively more phosphorus (P), potassium (K), and titanium (Ti), and a more prominent fluorine (F) peak were detected in some SEM spectra for CV ash (Figure 2).

Elemental mapping images for particles from both eruptions indicate that surficial Fe is often concentrated in discrete areas rather than being evenly distributed across the particle surface (Figure 3). The XRF and XPS analyses show depletion of Fe at the particle surface, with the Fe:Si ratio dropping from ~0.2 in the bulk to ~0.1 at the surface for La Soufrière and from ~0.6 to ~0.5 in the bulk to ~0.2 (for both) at the surface for both CV-West and CV-South (Tables S2 and S3 in Supporting Information S1). This is consistent with XPS and bulk Fe data for volcanic material reported by Delmelle et al. (2007) and Hornby et al. (2024). The CV-West and CV-South samples also have very high levels of surficial F with an average surficial F/Si atomic ratio of ~0.3 compared to ~0.02 in the La Soufrière sample (Table S3 in Supporting Information S1).

3.3. Fe-Specific Mineralogy

Fe in ash from both eruptions exists primarily as Fe(II) rather than Fe(III), as indicated by the wideset central doublet in the Mössbauer spectra (Figure 4).

Modeling of the experimental data and comparison to spectral parameters reported for pyroxenes in soils (Peretyazhko et al., 2012) and synthetic titanomagnetites (Pearce et al., 2012) indicates that the Fe contained in both

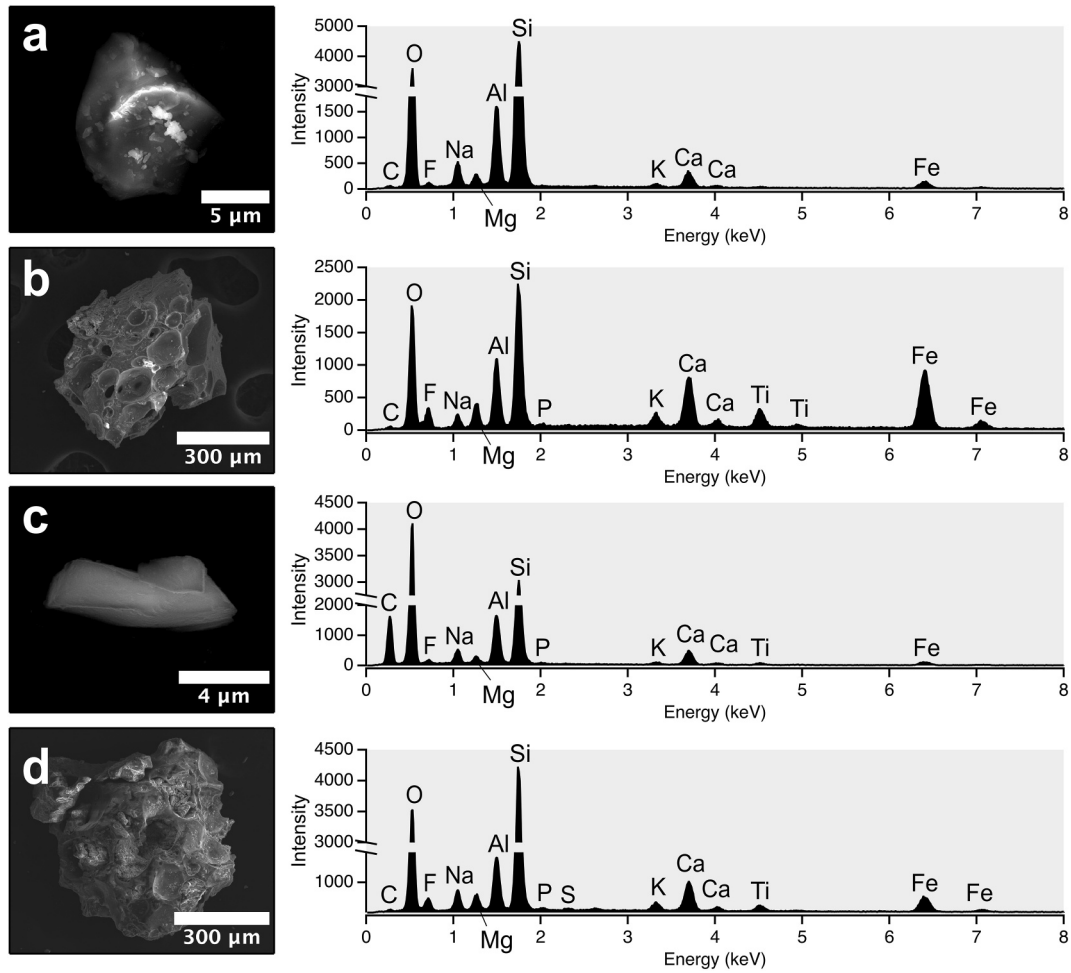

Figure 2. Scanning electron microscopy images of individual particles (left) from the La Soufrière eruption (a), Cumbre Vieja (CV)-East (b), CV-West (c), and CV-South (d) and their corresponding EDS spectra (right) indicating relative abundance of elements in the particle. Samples were mounted on a carbon substrate, so C and O signals in the EDS spectra are from the substrate rather than the particles.

the La Soufrière and the Cumbre Vieja (CV-West) ash is present in two main types of Fe-bearing minerals: clinopyroxene ($XY(Si,Al)_2O_6$), an Fe(II)- and Fe(III)-containing silicate, and Ti-containing oxides like ilmenite ($Fe(II)Ti(IV)O_4$) and Fe(II)/Fe(III)-titanomagnetite ($Fe_{3-x}Ti_xO_4$). X-ray diffraction analysis and comparison with previously published mineralogical data for the CV ash (Hornby et al., 2023) helped with specific identification of the crystalline phases (Text S8 in Supporting Information S1). About 56% of the total Fe in the La Soufrière sample is in clinopyroxene, and about 44% of the total Fe is in oxide minerals (Table 1). About 75% of the total Fe in the CV sample is contained in clinopyroxene, with only about 25% of the total Fe in oxides.

3.4. Particle Size

Microscopy analysis revealed that, while some larger particles (>~200 µm) exist, smaller particles (<~200 µm) are most abundant in ash samples from both eruptions (Figures S5 and S6 in Supporting Information S1). While ash from the La Soufrière eruption is more uniform in size and almost entirely falls into this range, some of the particles from the CV samples measure several hundreds of microns in diameter (Figure 2, Figure S6 in Supporting Information S1). However, these ultracoarse particles are largely irrelevant when considering deposition into the open ocean. Both volcanic vents are <10 km from the shore, but ash grainsize from magmatic eruptions can be reduced by a factor of ~4 for 20 km of transport for distances <80 km (Osman et al., 2020). Since particles <63 µm in diameter are relatively unaffected by fallout at the 10–100 km distance, our particle size distributions, which focus on particles up to 60 µm collected close the volcanic vents, should be comparable to the particle size

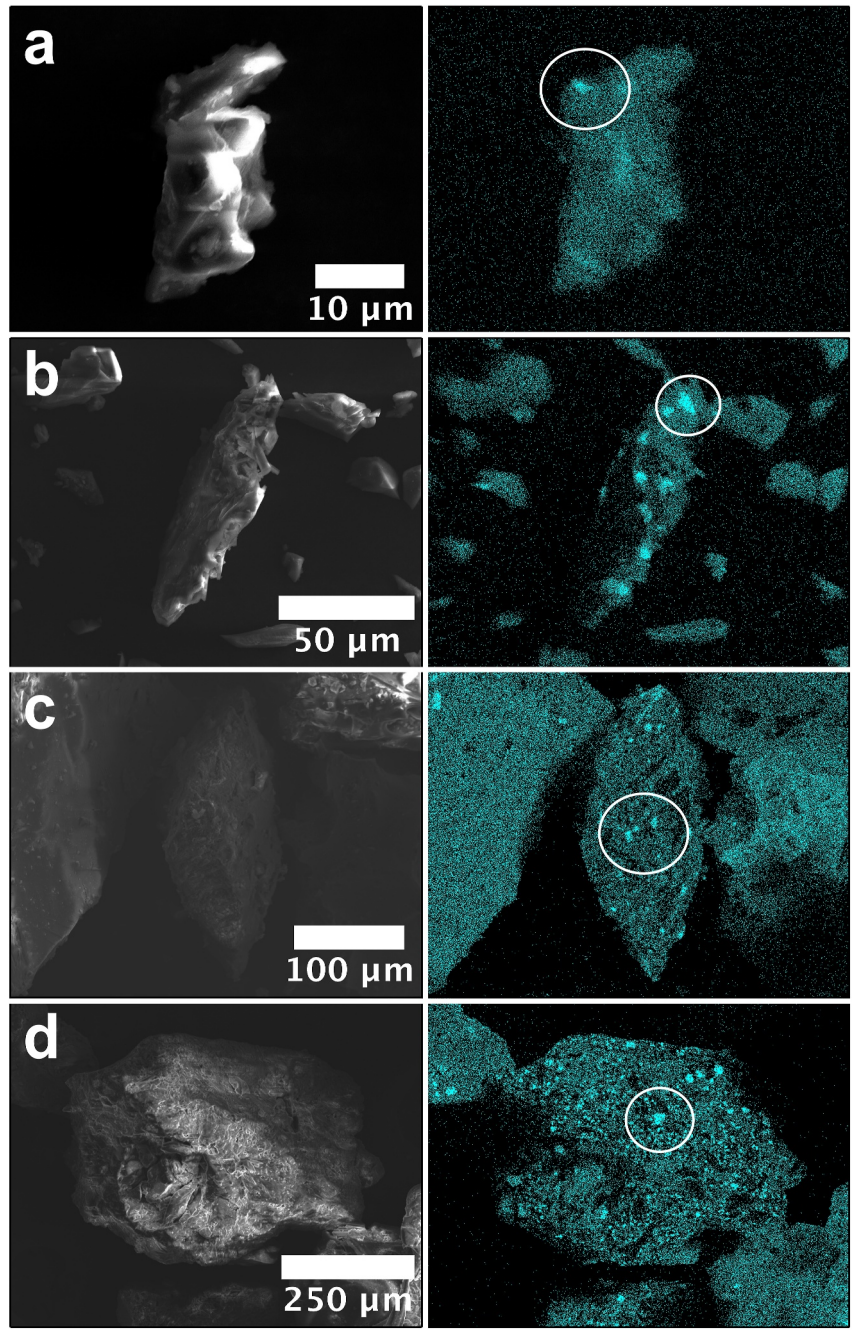

Figure 3. Scanning electron microscopy images (left) and EDX elemental maps (right) for individual particles from La Soufrière (a), Cumbre Vieja (CV)-East (b), CV-West (c), and CV-South (d). The cyan color indicates the location of Fe, with white circles highlighting examples of concentrated regions of Fe.

distributions that will be deposited into the North Atlantic, at least at 10 km of distance (Cashman & Rust, 2016). Furthermore, preliminary quantitative analysis with the Coulter Counter confirms that few particles exist beyond the ~60 µm size range (Figure S4 in Supporting Information S1). Based on our Coulter Counter analysis, the CV-East and CV-South samples have supermicron mode particle diameters (1.43 and 1.35 µm, respectively, from their log-normal fits; see Figure 5 for size distributions; see Figure S7 in Supporting Information S1 for error on replicate size measurements and blank data).

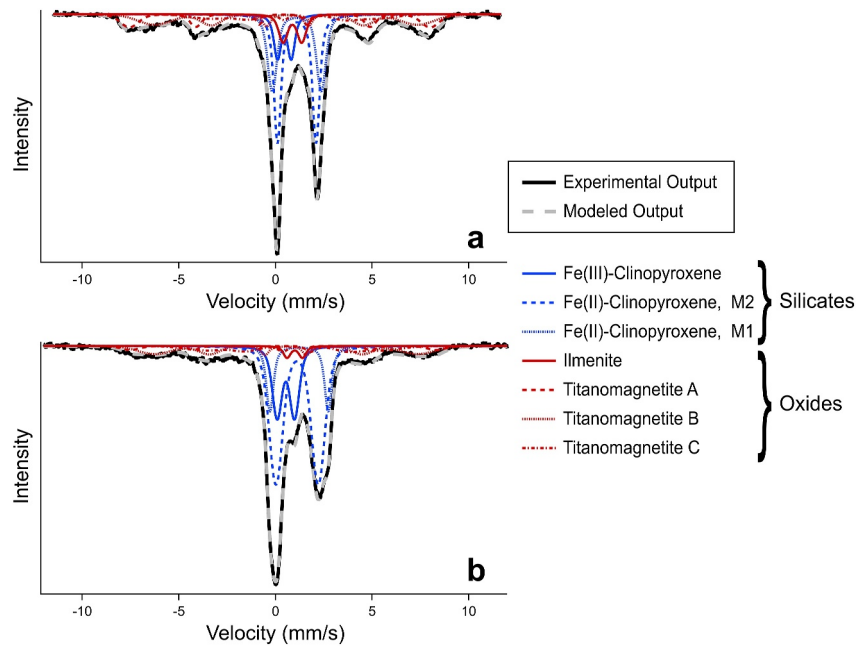

Figure 4. Experimental and modeled Mössbauer spectra for the La Soufrière sample at room temperature (a) and Cumbre Vieja-West at 225 K (b) modeled against outputs for various types of silicate (blue) and oxide (red) minerals.

The particle diameter modes are submicron for the La Soufrière and CV-West samples, so they are not visible in the Coulter Counter plots. Both particle diameter modes were estimated to be roughly 115 nm based on NTA of a different ash sample produced by the La Soufrière eruption with a comparable supermicron size distribution (Figures S8 and S9 in Supporting Information S1).

4. Discussion

Our results show that the total Fe content and soluble Fe content in different types of volcanic ash are variable. The total Fe content in the CV samples is, on average, ~1.8 times that of the La Soufrière ash. The average soluble Fe content in the CV ash is ~4.9 times that of La Soufrière ash, leading to average fractional solubility estimates of 3.6% ± 2.1% and 1.3% for Fe in ash from the two eruptions. Our solubility estimates are higher than the estimates for Fe fractional solubility in volcanic ash reported in previous studies (<0.01–1%; Ayris & Delmelle, 2012; Duggen et al., 2010; Olgun et al., 2011), possibly due to the rigor of our leaching procedure, which is meant to provide an upper limit for Fe solubility (Shelley et al., 2018). Our results confirm that bulk Fe content does not directly correlate to soluble Fe content for volcanic material (Olgun et al., 2011), and thus bulk Fe concentration cannot be used to estimate the potential for release of ash-derived soluble Fe into surface waters. Notably, the CV-East sample, which may have lost soluble Fe if salt coatings containing Fe on the ash particle surfaces dissolved when the sample was exposed to rain (Capitani et al., 2018; Duggen et al., 2010; Jones & Gislason, 2008; Olgun et al., 2011), had an intermediate soluble Fe level compared to the other two CV samples, and was included in the analysis since results were typical for ash from this eruption.

Table 1
Estimates for Percent of Total Fe in the La Soufrière and Cumbre Vieja (CV)-West Samples Contained in Different Minerals (Determined Using Mössbauer Spectroscopy-Room Temperature Mössbauer Spectroscopy for the Soufrière Sample; 225 K Mössbauer Spectroscopy for the CV-West Sample)

	% Of total Fe contained in mineral	
Mineral	La Soufrière (%)	CV-west (%)
Fe(II)-clinopyroxene, M1 and M2	47.2	57.6
Fe(III)-clinopyroxene	9.2	17.2
Titanomagnetite	36.9	22.9
Ilmenite	6.9	2.3
Total %Fe in silicates:	~56	~75
Total %Fe in oxides:	~44	~25

Ash composition primarily explains the observed difference in Fe solubility. Elemental mapping showed that the particles either had heterogeneous mineralogy throughout or unevenly distributed Fe-containing surficial deposits. Modeling of Mössbauer spectra revealed that the majority of Fe in both La Soufrière and CV-West ash is contained within clinopyroxene and oxides (primarily titanomagnetite). This is supported by previous X-ray diffraction analysis showing pyroxene and Fe oxides in ash deposits from the CV

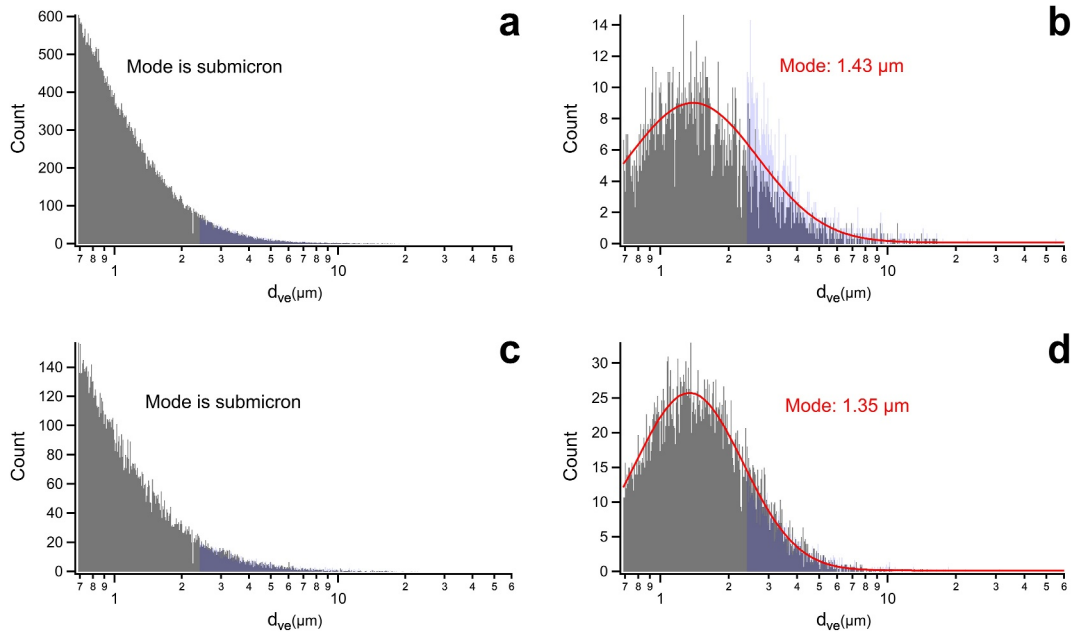

Figure 5. Particle size data as volume equivalent diameter (d_{ve}) for La Soufrière (a), Cumbre Vieja (CV)-East (b), CV-West (c), and CV-South (d), measured using the 30 and 100 μm apertures with a Coulter Counter. Grey bars indicate size data acquired using the 30-μm aperture. Transparent purple bars indicate the size data acquired using the 100-μm aperture. Red lines are log-normal fits to the data for the samples with supermicron modes.

eruption (Hornby et al., 2023). Fe in aluminosilicate minerals like clinopyroxene, possibly present as Fe(II) substitutions, tends to be more soluble than Fe in (hydr-)oxides where it is held by strong covalent bonds (Chen et al., 2012; Cwiertny et al., 2008; Journet et al., 2008). 75% of the total Fe in the CV-West ash was found to be in silicate minerals where it should be relatively soluble. Only 56% of the total Fe in the La Soufrière ash is in silicates, with the remaining 44% in oxides and less likely to be released into solution.

Mineralogical differences in magma produced by the different eruptions cannot be the only control on Fe solubility. Both the most and least soluble CV samples, CV-West and CV-South, contain about 1.8 times the total Fe content of La Soufrière ash but about 8 and 2.5 times its soluble Fe content, respectively, which implies that another factor must be impacting Fe dissolution among samples from the same eruption. High levels of fluorine (F) have been linked to elevated Fe release from volcanic ash, likely because F remains on the surface after particles have been processed through interaction with liquid- and gas-phase hydrofluoric acid (HF) in the volcanic plume (Ayris & Delmelle, 2012; Delmelle et al., 2007; Hoshyaripour et al., 2015; Jones & Gislason, 2008; Óskarsson, 1980). Interactions with acids and water in the volcanic plume are thought to dissolve volcanic glass, creating a deliquescent layer, largely composed of sulphate and halide deposits, on the particle surface that would have been solubilized upon deposition into seawater or during our leaching (Delmelle et al., 2007; Duggen et al., 2010; Óskarsson, 1980). These surficial deposits are very thin (<10 nm) but can contain Fe salts that will readily dissolve, increasing total soluble Fe release from an ash sample (Delmelle et al., 2007; Duggen et al., 2010). The amount of surficial, highly soluble F (and, presumably the thickness of the deliquescent layer) is likely linked to the duration of exposure to the volcanic plume and its acidity, so we expect higher F levels to be correlated with more readily soluble surficial Fe (Hoshyaripour et al., 2015; Óskarsson, 1980). Compared to La Soufrière, we measured elevated levels of surficial F in CV samples, indicating that they have likely been exposed to higher concentrations of HF. We also measured differences in surficial F content between samples from the CV eruption, and Fe solubility tracks relatively well with surficial F. We measured a surficial F content (At%) of 6.6% for CV-West, and Fe solubility for this sample was 5.9%. For CV-South, both surficial F content (2.2%) and Fe solubility (1.9%) were much lower, suggesting that plume chemistry is a major factor impacting Fe dissolution (Hoshyaripour et al., 2015; Maters et al., 2017).

While the distribution of total Fe between mineral groups and surficial F levels can explain the observed differences in Fe solubility, particle size appears to have a less significant impact. Theoretically, finer particles with

higher surface area-to-volume (SA:V) ratios should release more soluble Fe into solution, especially if soluble Fe is primarily contained in surficial salts (Baker & Jickells, 2006; Jones & Gislason, 2008; Langmann et al., 2010). We found that particles from the CV-East and CV-South samples are generally larger than La Soufrière ash particles (and up to hundreds of microns in diameter) but contain ∼4.4 and ∼2.5 times the soluble Fe content of ash from that eruption, implying that particle size cannot be a primary control on soluble Fe release. Among the three samples from the CV eruption, the CV-West sample, which has the smallest mode particle size of the CV samples for the size range analyzed by the Coulter Counter, has the highest soluble Fe content (∼1.8 and ∼3.3 times the soluble Fe content of the other CV samples). However, since the CV-West sample also has very high surficial F content, we cannot conclusively link its smaller mode particle size to enhanced Fe solubility.

Our soluble Fe content and solubility estimates for volcanic ash from the Eyjafjallajökull eruption are comparable to our estimates for ash from the 2021 eruptions. However, we found that the average soluble Fe content in our mineral dust samples collected in Barbados during June 2020 was about 1.5 times that of the four ash samples analyzed in this study, despite only containing about half of the average total Fe in the ash. We estimate that Fe in mineral dust is about 9.3 ± 1.4% soluble, compared to 3.0 ± 2.0% soluble, on average, in ash from La Soufrière and CV. Ayris and Delmelle (2012) previously reported that Fe fractional solubilities measured for mineral dust (generally 1% or higher; Jickells & Spokes, 2001) are higher than those reported for volcanic ash. Our solubility estimate for Fe in mineral dust is higher than some other estimates (like the 1%–2% estimate from Jickells & Spokes, 2001), but the leach employed here provides an upper estimate for Fe solubility (Shelley et al., 2018). Our estimate is comparable to that of Shelley et al. (2018), who reported an Fe fractional solubility of 6.4 ± 1.0% using the Berger et al. (2008) leach for aerosols identified as North African in origin. This solubility estimate is still higher than the average we report for our ash samples, indicating that a higher proportion of the Fe in ash is refractory in nature (not released using the Berger leach). It remains unclear why Fe solubility is higher in dust compared to ash in general, but this topic is difficult to investigate since ash from different eruptions varies significantly in composition. Clay minerals have been identified as an important source of soluble Fe in dust aerosols (Jeong & Achterberg, 2014; Journet et al., 2008); therefore, differences in the type and structure of clay minerals present in dust and ash may be partially responsible for the observed differences in Fe solubility.

The potential of an aerosol source to add nutrients to the surface ocean depends on both the soluble nutrient content and total mass of aerosol deposited. Both factors must be considered when comparing soluble Fe inputs from different sources. Yu et al. (2015) estimated that, within a strip spanning from 10°S to 30°N, 182 Tg dust is carried westward from North Africa across 15°W longitude, while only about 43 Tg dust reaches 75°W longitude each year. Errors in these estimates are discussed in Yu et al. (2015). Based on Yu et al. (2015)'s data, we estimate that about 139 Tg of mineral dust from North Africa (based on the difference in dust mass from the two longitudes) is deposited into the North Atlantic annually (Yu et al., 2015). Although Yu et al. (2015)'s values are derived from 7 years of data and annual dust fluxes vary significantly, this estimate is reasonable based on other estimates of annual dust deposition into the North Atlantic (Ginoux et al., 2004; Prospero, 1996). Using our estimate for soluble Fe release, this amounts to 0.53 Tg of soluble Fe deposition annually from mineral dust. While dust deposition follows a regular annual cycle, volcanic eruptions are much less predictable and only occasionally lead to significant deposition in the North Atlantic (Husar et al., 1997; Prospero & Lamb, 2003; Zuidema et al., 2019). Based on data on eruptions from 1980 to 2019 from Galetto et al. (2023), we estimate that about 40.6–64.8 Tg of explosive volcanic products are produced by volcanoes situated in/around the North Atlantic annually (Text S11 in Supporting Information S1). Assuming that the ash has a soluble Fe content of approximately the average for the four samples from La Soufrière and CV analyzed in this study, that much ash deposition amounts to about 0.11–0.17 Tg of volcanic-derived soluble Fe deposited per year (∼20–32% of our estimated annual deposition from mineral dust). Volcanic ash, therefore, may provide an important additional annual contribution to the North Atlantic's soluble Fe budget.

Despite its relative unimportance on long temporal scales, volcanic eruptions may have the potential to stimulate localized phytoplankton blooms, as has been previously proposed (Hamme et al., 2010; Langmann et al., 2010; Vergara-Jara et al., 2021), because they can provide large fluxes of material to regions that do not receive appreciable Fe inputs from mineral dust. Ash-derived Fe inputs may be especially important, for example, in the northeastern Atlantic Basin near western Europe, where Fe is thought to be the primary limiting nutrient (Moore et al., 2013). Similarly, ash-derived Fe inputs to the subtropical North Atlantic will likely be more important if eruptions occur during boreal winter, when mineral dust concentrations in air are relatively low at this latitude (Adams et al., 2012; Zuidema et al., 2019).

Our soluble Fe measurements, the known eruption lengths (Joseph et al., 2022; Milford et al., 2023), and our calculated eruption-specific deposition velocities allow us to estimate ash-derived dissolved Fe (DFe) inputs to the mixed layer during the La Soufrière and CV eruptions specifically, assuming that the airborne ash concentration over affected regions of the North Atlantic was 61 $\mu g/m^3$ during both eruptive events (Milford et al., 2023) and the mixed layer depth was 20 m (see Text S12 in Supporting Information S1 for details about the calculations). For these calculations, we did not consider mixed layer depth fluctuations or changes in wind currents and atmospheric transport. We assume that the ash deposited into the ocean has the same soluble Fe content that we measured in the bulk ash samples, with an average of the three samples used for CV. Using our particle mode size data and a density of ~2.71 g/cm^3 for the La Soufrière ash and ~3.00 g/cm^3 for the CV ash (Hornby et al., 2023; see Text S12 and Table S4 in Supporting Information S1 for density calculations) to calculate eruption-specific particle deposition velocities using the Stokes' equation for settling velocity (Barkley et al., 2021; Huang et al., 2020), we estimate that the La Soufrière eruption increased DFe concentrations in the mixed layer by ~0.05 pM over a 14-day eruption (Joseph et al., 2022), while the CV eruption increased DFe by ~0.1 nM over an 86-day eruptive period (Milford et al., 2023; see Text S12 in Supporting Information S1 for deposition velocity and DFe calculations). Whether or not these DFe concentrations will actually be available for microbial uptake remains unclear. While several biotic and abiotic processes control Fe levels in the upper ocean, aerosol-derived Fe, particularly solubilized Fe(II) which is rapidly oxidized in seawater, is thought to be largely present as colloidal-sized precipitates which aggregate to form sinking authigenic particles through a "colloidal shunt" (Tagliabue et al., 2023). Aerosol-derived fertilization of the surface ocean will only be biologically relevant if existing nutrient inventories in surface waters are low. Since both eruptions impacted regions where background DFe concentrations can be <1 nM during the seasons in which the eruptions occurred, even small perturbations to the marine Fe cycle may be biologically relevant (Sarthou et al., 2007; Sedwick et al., 2020).

5. Conclusions

Our results provide insight about the potential significance of volcanic ash as a regionally important soluble Fe source. The CV eruption produced larger, more mafic ash particles with Fe primarily contained in silicate minerals and high levels of surficial F. Ash with these characteristics is more likely to provide a large enough flux of soluble Fe to surface waters near the eruption site to cause a phytoplankton bloom. On the other hand, the La Soufrière eruption produced smaller, more silicic ash particles with a higher percentage of the total Fe in oxides and less surficial F. This type of ash will not be rapidly deposited close to the source and does not contain enough soluble Fe to notably increase DFe concentration, given its relatively slow deposition rate. Our estimates demonstrate that, while chemical composition dictates Fe solubility in volcanic material, the deposition rate and baseline DFe concentrations in the receiving system inevitably determine the biological impact of volcanic Fe inputs. When all of these factors are considered, it is evident that volcanic eruptions are unique events that must be studied within the context of the surrounding environment. These findings, combined with biases in remote sensing, can help explain why different studies have documented disparate marine microbial responses to volcanic ash deposition.

Acknowledgments
CJG acknowledges funding from an NSF CAREER Grant (AGS-1944958) and a user proposal (#51900) from the Environmental Molecular Sciences Laboratory at the Pacific Northwest National Laboratory sponsored by the Office of Biological and Environmental Research of the U.S. Department of Energy. HEE acknowledges the University of Miami Graduate School Dean's Fellowship. Particle size analysis was supported by the University of Michigan College of Literature Science and the Arts "Meet the Moment" Initiative. APA was funded by the NIH/NSF Oceans and Human Health Center program (2P01ES028939-06), while RLP was supported by an NSF graduate research fellowship (DGE-2241144). We thank Ali Pourmand, Arash Sharifi, and Amanda Oehlert for assistance with sample digestion and use of laboratory space.

Global Research Collaboration

We thank the family of HC Manning and the Herbert C Manning Trust for providing access to their land at Ragged Point in Barbados and collaborators at the Barbados Atmospheric Chemistry Observatory (BACO) for collecting and providing volcanic ash and mineral dust for our analysis. We also thank Plan de Emergencias Volcánicas de Canarias (PEVOLCA) for enabling sample collection in the exclusion zone on La Palma during the 2021 CV eruption.

Data Availability Statement

The total Fe, soluble Fe, and particle size data used in the study are available in the University of Miami data repository at https://scholarship.miami.edu/esploro/outputs/991032699646602976 (Elliott et al., 2025).

References

Adams, A. M., Prospero, J. M., & Zhang, C. (2012). CALIPSO-derived three-dimensional structure of aerosol over the Atlantic Basin and adjacent continents. *Journal of Climate*, *25*(19), 6862–6879. https://doi.org/10.1175/JCLI-D-11-00672.1

Allen, T. (2003). Stream scanning methods of particle size measurement. In R. Davies (Ed.), *Powder sampling and particle size determination* (pp. 447–523). Elsevier Science & Technology.

Ault, A. P., Peters, T. M., Sawvel, E. J., Casuccio, G. S., Willis, R. D., Norris, G. A., & Grassian, V. H. (2012). Single-particle SEM-EDX analysis of iron-containing coarse particulate matter in an urban environment: Sources and distribution of iron within Cleveland, Ohio. *Environmental Science & Technology*, *46*(8), 4331–4339. https://doi.org/10.1021/es204006k

Axson, J. L., Creamean, J. M., Bondy, A. L., Capracotta, S. S., Warner, K. Y., & Ault, A. P. (2015). An in situ method for sizing insoluble residues in precipitation and other aqueous samples. *Aerosol Science and Technology*, *49*(1), 24–34. https://doi.org/10.1080/02786826.2014.991439

Ayris, P., & Delmelle, P. (2012). Volcanic and atmospheric controls on ash iron solubility: A review. *Physics and Chemistry of the Earth Parts A/B/C*, *45–46*, 103–112. https://doi.org/10.1016/j.pce.2011.04.013

Bains, S., Norris, R. D., Corfield, R. M., & Faul, K. L. (2000). Termination of global warmth at the Palaeocene/Eocene boundary through productivity feedback. *Nature*, *407*(6801), 171–174. https://doi.org/10.1038/35025035

Baker, A. R., & Croot, P. L. (2010). Atmospheric and marine controls on aerosol iron solubility in seawater. *Marine Chemistry*, *120*(1), 4–13. https://doi.org/10.1016/j.marchem.2008.09.003

Baker, A. R., & Jickells, T. D. (2006). Mineral particle size as a control on aerosol iron solubility. *Geophysical Research Letters*, *33*(17), L17608. https://doi.org/10.1029/2006GL026557

Barkley, A. E., Olson, N. E., Prospero, J. M., Gatineau, A., Panechou, K., Maynard, N. G., et al. (2021). Atmospheric transport of North African dust-bearing supermicron freshwater diatoms to South America: Implications for iron transport to the equatorial North Atlantic Ocean. *Geophysical Research Letters*, *48*(5), 12. https://doi.org/10.1029/2020GL090476

Bay, R. C., Bramall, N., & Price, P. B. (2004). Bipolar correlation of volcanism with millennial climate change. *PNAS*, *101*(17), 6341–6345. https://doi.org/10.1073/pnas.0400323101

Berger, C. J. M., Lippiatt, S. M., Lawrence, M. G., & Bruland, K. W. (2008). Application of a chemical leach technique for estimating labile particulate aluminum, iron, and manganese in the Columbia River plume and coastal waters off Oregon and Washington. *Journal of Geophysical Research C Oceans*, *113*(C2), C00B01. https://doi.org/10.1029/2007JC004703

Bisson, K. M., Gasso, S., Mahowald, N., Wagner, S., Koffman, B., Carn, S. A., et al. (2023). Observing ocean ecosystem responses to volcanic ash. *Remote Sensing of Environment*, *296*, 113749. https://doi.org/10.1016/j.rse.2023.113749

Browning, T. J., Stone, K., Bouman, H. A., Mather, T. A., Pyle, D. M., Moore, C. M., & Martinez-Vicente, V. (2015). Volcanic ash supply to the surface ocean—Remote sensing of biological responses and their wider biogeochemical significance. *Frontiers in Marine Science*, *2*, 1–22. https://doi.org/10.3389/fmars.2015.00014

Buck, C. S., Landing, W. M., & Resing, J. A. (2010). Particle size and aerosol iron solubility: A high-resolution analysis of Atlantic aerosols. *Marine Chemistry*, *120*(1), 14–24. https://doi.org/10.1016/j.marchem.2008.11.002

Caballero, I., Román, A., Tovar-Sánchez, A., & Navarro, G. (2022). Water quality monitoring with Sentinel-2 and Landsat-8 satellites during the 2021 volcanic eruption in La Palma (Canary Islands). *The Science of the Total Environment*, *822*, 153433. https://doi.org/10.1016/j.scitotenv.2022.153433

Capitani, G., Miyajima, N., Sulpizio, R., D'Addabbo, M., Galimberti, L., Guidi, M., & Andreozzi, G. B. (2018). Iron release in aqueous environment by fresh volcanic ash from Mount Etna (Italy) and Popocatépetl (Mexico) volcanoes. *Environmental Earth Sciences*, *77*(13), 1–15. https://doi.org/10.1007/s12665-018-7692-z

Cashman, K., & Rust, A. (2016). Part 2: Volcanic ash: Generation and spatial variations. In S. Mackie, H. Ricketts, M. Watson, K. Cashman, & A. Rust (Eds.), *Volcanic ash: Hazard observation* (pp. 5–22). Elsevier Inc. https://doi.org/10.1016/B978-0-08-100405-0.00002-1

Chen, H., Laskin, A., Baltrusaitis, J., Gorski, C. A., Scherer, M. M., & Grassian, V. H. (2012). Coal fly ash as a source of iron in atmospheric dust. *Environmental Science & Technology*, *46*(4), 2112–2120. https://doi.org/10.1021/es204102f

Chester, R., & Hughes, M. J. (1967). A chemical technique for the separation of ferro-manganese minerals, carbonate minerals and adsorbed trace elements from pelagic sediments. *Chemical Geology*, *2*, 249–262. https://doi.org/10.1016/0009-2541(67)90025-3

Claustre, H., Morel, A., Hooker, S. B., Babin, M., Antoine, D., Oubelkheir, K., et al. (2002). Is desert dust making oligotrophic waters greener? *Geophysical Research Letters*, *29*(10), 107-1–107-4. https://doi.org/10.1029/2001GL014056

Creamean, J. M., Axson, J. L., Bondy, A. L., Craig, R. L., May, N. W., Shen, H., et al. (2016). Changes in precipitating snow chemistry with location and elevation in the California Sierra Nevada. *Journal of Geophysical Research: Atmospheres*, *121*(12), 7296–7309. https://doi.org/10.1002/2015JD024700

Cwiertny, D. M., Baltrusaitis, J., Hunter, G. J., Laskin, A., Scherer, M. M., & Grassian, V. H. (2008). Characterization and acid-mobilization study of iron-containing mineral dust source materials. *Journal of Geophysical Research. D. (Atmospheres)*, *113*(D5), D05202. https://doi.org/10.1029/2007JD009332

Delmelle, P., Lambert, M., Dufrêne, Y., Gerin, P., & Óskarsson, N. (2007). Gas/aerosol–ash interaction in volcanic plumes: New insights from surface analyses of fine ash particles. *Earth and Planetary Science Letters*, *259*(1), 159–170. https://doi.org/10.1016/j.epsl.2007.04.052

De Luca, C., Valerio, E., Giudicepietro, F., Macedonio, G., Casu, F., & Lanari, R. (2022). Pre- and co-eruptive analysis of the September 2021 eruption at Cumbre Vieja Volcano (La Palma, Canary Islands) through DInSAR measurements and analytical modeling. *Geophysical Research Letters*, *49*(7), e2021GL097293. https://doi.org/10.1029/2021GL097293

Duggen, S., Olgun, N., Croot, P., Hoffmann, L., Dietze, H., Delmelle, P., & Teschner, C. (2010). The role of airborne volcanic ash for the surface ocean biogeochemical iron-cycle: A review. *Biogeosciences*, *7*(3), 827–844. https://doi.org/10.5194/bg-7-827-2010

Elliott, H. E., Blades, E., Royer, H. M., Buck, C., Kollman, C., Kukkadapu, R., et al. (2025). Composition and plume gas interaction control iron fractional solubility more than particle size in volcanic ash: Implications for fertilization of the North Atlantic [Dataset]. *University of Miami Libraries*. https://doi.org/10.17604/x1n6-r149

Elliott, H. E., Popendorf, K. J., Blades, E., Royer, H. M., Pollier, C. G. L., Oehlert, A. M., et al. (2024). Godzilla mineral dust and La Soufrière volcanic ash fallout immediately stimulate marine microbial phosphate uptake. *Frontiers in Marine Science*, *10*, 1308689. https://doi.org/10.3389/fmars.2023.1308689

Galetto, F., Pritchard, M. E., Hornby, A. J., Gazel, E., & Mahowald, N. M. (2023). Spatial and temporal quantification of subaerial volcanism from 1980 to 2019: Solid products, masses, and average eruptive rates. *Reviews of Geophysics*, *61*(1), e2022RG000783. https://doi.org/10.1029/2022RG000783

Geisen, C., Ridame, C., Journet, E., Delmelle, P., Marie, D., Lo Monaco, C., et al. (2022). Phytoplanktonic response to simulated volcanic and desert dust deposition events in the South Indian and Southern Oceans. *Limnology & Oceanography*, *67*(7), 1537–1553. https://doi.org/10.1002/lno.12100

Ginoux, P., Prospero, J. M., Torres, O., & Chin, M. (2004). Long-term simulation of global dust distribution with the GOCART model: Correlation with North Atlantic Oscillation. *Environmental Modelling & Software: With Environment Data News*, *19*(2), 113–128. https://doi.org/10.1016/S1364-8152(03)00114-2

Gislason, S. R., Hassenkam, T., Nedel, S., Bovet, N., Eiriksdottir, E. S., Alfredsson, H. A., et al. (2011). Characterization of Eyjafjallajökull volcanic ash particles and a protocol for rapid risk assessment. *Proceedings of the National Academy of Sciences*, *108*(18), 7307–7312. https://doi.org/10.1073/pnas.1015053108

Hamme, R. C., Webley, P. W., Crawford, W. R., Whitney, F. A., DeGrandpre, M. D., Emerson, S. R., et al. (2010). Volcanic ash fuels anomalous plankton bloom in subarctic northeast Pacific. *Geophysical Research Letters*, *37*(19), L19604. https://doi.org/10.1029/2010GL044629

Hoffmann, L. J., Breitbarth, E., Ardelan, M. V., Duggen, S., Olgun, N., Hassellöv, M., & Wängberg, S.-Å. (2012). Influence of trace metal release from volcanic ash on growth of *Thalassiosira pseudonana* and *Emiliania huxleyi*. *Marine Chemistry*, *132–133*, 28–33. https://doi.org/10.1016/j.marchem.2012.02.003

Hoover, B. M., & Murphy, R. M. (2020). Evaluation of nanoparticle tracking analysis for the detection of rod-shaped particles and protein aggregates. *Journal of Pharmaceutical Sciences*, *109*(1), 452–463. https://doi.org/10.1016/j.xphs.2019.10.006

Hornby, A. J., Ayris, P. M., Damby, D. E., Diplas, S., Eychenne, J., Kendrick, J. E., et al. (2024). Nanoscale silicate melt textures determine volcanic ash surface chemistry. *Nature Communications*, *15*(1), 531. https://doi.org/10.1038/s41467-024-44712-6

Hornby, A. J., Gazel, E., Bush, C., Dayton, K., & Mahowald, N. (2023). Phases in fine volcanic ash. *Scientific Reports*, *13*(1), 15728. https://doi.org/10.1038/s41598-023-41412-x

Hoshyaripour, G., Hort, M., Langmann, B., & Delmelle, P. (2014). Volcanic controls on ash iron solubility: New insights from high-temperature gas–ash interaction modeling. *Journal of Volcanology and Geothermal Research*, *286*, 67–77. https://doi.org/10.1016/j.jvolgeores.2014.09.005

Hoshyaripour, G. A., Hort, M., & Langmann, B. (2015). Ash iron mobilization through physicochemical processing in volcanic eruption plumes: A numerical modeling approach. *Atmospheric Chemistry and Physics*, *15*(16), 9361–9379. https://doi.org/10.5194/acp-15-9361-2015

Huang, Y., Kok, J. F., Kandler, K., Lindqvist, H., Nousiainen, T., Sakai, T., et al. (2020). Climate models and remote sensing retrievals neglect substantial desert dust asphericity. *Geophysical Research Letters*, *47*(6), e2019GL086592. https://doi.org/10.1029/2019GL086592

Husar, R. B., Prospero, J. M., & Stowe, L. L. (1997). Characterization of tropospheric aerosols over the oceans with the NOAA advanced very high resolution radiometer optical thickness operational product. *Journal of Geophysical Research*, *102*(D14), 16889–16909. https://doi.org/10.1029/96JD04009

Jeong, G. Y., & Achterberg, E. P. (2014). Chemistry and mineralogy of clay minerals in Asian and Saharan dusts and the implications for iron supply to the oceans. *Atmospheric Chemistry and Physics*, *14*(22), 12415–12428. https://doi.org/10.5194/acp-14-12415-2014

Jicha, B. R., Scholl, D. W., & Rea, D. K. (2009). Circum-Pacific arc flare-ups and global cooling near the Eocene-Oligocene boundary. *Geology*, *37*(4), 303–306. https://doi.org/10.1130/G25392A.1

Jickells, T. D., & Spokes, L. J. (2001). Atmospheric iron input to the ocean. In D. R. Turner & K. A. Hunter (Eds.), *The biogeochemistry of iron in seawater* (p. 401). John Wiley and Sons Ltd.

Jones, M. T., & Gislason, S. R. (2008). Rapid releases of metal salts and nutrients following the deposition of volcanic ash into aqueous environments. *Geochimica et Cosmochimica Acta*, *72*(15), 3661–3680. https://doi.org/10.1016/j.gca.2008.05.030

Joseph, E. P., Camejo-Harry, M., Christopher, T., Contreras-Arratia, R., Edwards, S., Graham, O., et al. (2022). Responding to eruptive transitions during the 2020–2021 eruption of La Soufrière volcano, St. Vincent. *Nature Communications*, *13*(1), 4129. https://doi.org/10.1038/s41467-022-31901-4

Journet, E., Desboeufs, K. V., Caquineau, S., & Colin, J.-L. (2008). Mineralogy as a critical factor of dust iron solubility. *Geophysical Research Letters*, *35*(7), L07805. https://doi.org/10.1029/2007GL031589

Langmann, B., Zakšek, K., Hort, M., & Duggen, S. (2010). Volcanic ash as fertilizer for the surface ocean. *Atmospheric Chemistry and Physics*, *10*(8), 3891–3899. https://doi.org/10.5194/acp-10-3891-2010

Maters, E. C., Delmelle, P., & Gunnlaugsson, H. P. (2017). Controls on iron mobilisation from volcanic ash at low pH: Insights from dissolution experiments and Mössbauer spectroscopy. *Chemical Geology*, *449*, 73–81. https://doi.org/10.1016/j.chemgeo.2016.11.036

Meskhidze, N., Völker, C., Al-Abadleh, H. A., Barbeau, K., Bressac, M., Buck, C., et al. (2019). Perspective on identifying and characterizing the processes controlling iron speciation and residence time at the atmosphere-ocean interface. *Marine Chemistry*, *217*(C), 103704. https://doi.org/10.1016/j.marchem.2019.103704

Milford, C., Torres, C., Vilches, J., Gossman, A.-K., Weis, F., Suárez-Molina, D., et al. (2023). Impact of the 2021 La Palma volcanic eruption on air quality: Insights from a multidisciplinary approach. *The Science of the Total Environment*, *869*, 161652. https://doi.org/10.1016/j.scitotenv.2023.161652

Moore, C. M., Mills, M. M., Arrigo, K. R., Berman-Frank, I., Bopp, L., Boyd, P. W., et al. (2013). Processes and patterns of oceanic nutrient limitation. *Nature Geoscience*, *6*(9), 701–710. https://doi.org/10.1038/ngeo1765

Myriokefalitakis, S., Ito, A., Kanakidou, M., Nenes, A., Krol, M. C., Mahowald, N. M., et al. (2018). Reviews and syntheses: The GESAMP atmospheric iron deposition model intercomparison study. *Biogeosciences*, *15*(21), 6659–6684. https://doi.org/10.5194/bg-15-6659-2018

Oakes, M., Ingall, E. D., Lai, B., Shafer, M. M., Hays, M. D., Liu, Z. G., et al. (2012). Iron solubility related to particle sulfur content in source emission and ambient fine particles. *Environmental Science & Technology*, *46*(12), 6637–6644. https://doi.org/10.1021/es300701c

Olgun, N., Duggen, S., Croot, P. L., Delmelle, P., Dietze, H., Schacht, U., et al. (2011). Surface ocean iron fertilization: The role of airborne volcanic ash from subduction zone and hot spot volcanoes and related iron fluxes into the Pacific Ocean: Volcanic ash-an ATMOSPHERIC FE SOURCE. *Global Biogeochemical Cycles*, *25*(4), GB4001. https://doi.org/10.1029/2009GB003761

Óskarsson, N. (1980). The interaction between volcanic gases and tephra: Fluorine adhering to tephra of the 1970 Hekla eruption. *Journal of Volcanology and Geothermal Research*, *8*(2–4), 251–266. https://doi.org/10.1016/0377-0273(80)90107-9

Osman, S., Beckett, F., Rust, A., & Snee, E. (2020). Sensitivity of volcanic ash dispersion modelling to input grain size distribution based on hydromagmatic and magmatic deposits. *Atmosphere*, *11*(6), 567. https://doi.org/10.3390/atmos11060567

Pearce, C. I., Qafoku, O., Liu, J., Arenholz, E., Heald, S. M., Kukkadapu, R. K., et al. (2012). Synthesis and properties of titanomagnetite ($Fe_{3-x}TixO_4$) nanoparticles: A tunable solid-state Fe(II/III) redox system. *Journal of Colloid and Interface Science*, *387*(1), 24–38. https://doi.org/10.1016/j.jcis.2012.06.092

Peretyazhko, T. S., Zachara, J. M., Kukkadapu, R. K., Heald, S. M., Kutnyakov, I. V., Resch, C. T., et al. (2012). Pertechnetate (TcO_4^-) reduction by reactive ferrous iron forms in naturally anoxic, redox transition zone sediments from the Hanford Site, USA. *Geochimica et Cosmochimica Acta*, *92*, 48–66. https://doi.org/10.1016/j.gca.2012.05.041

Perron, M. M. G., Strzelec, M., Gault-Ringold, M., Proemse, B. C., Boyd, P. W., & Bowie, A. R. (2020). Assessment of leaching protocols to determine the solubility of trace metals in aerosols. *Talanta*, *208*, 120377. https://doi.org/10.1016/j.talanta.2019.120377

Prospero, J. M. (1996). Saharan dust transport over the North Atlantic Ocean and Mediterranean: An overview. In S. Guerzoni & R. Chester (Eds.), *The impact of desert dust across the Mediterranean* (pp. 133–151). Springer.

Prospero, J. M., Bullard, J. E., & Hodgkins, R. (2012). High-Latitude dust over the North Atlantic: Inputs from Icelandic proglacial dust storms. *Science*, *335*(6072), 1078–1082. https://doi.org/10.1126/science.1217447

Prospero, J. M., & Lamb, P. J. (2003). African droughts and dust transport to the Caribbean: Climate change implications. *Science*, *302*(5647), 1024–1027. https://doi.org/10.1126/science.1089915

Rancourt, D. G., & Ping, J. Y. (1991). Voigt-based methods for arbitrary-shape static hyperfine parameter distributions in Mössbauer spectroscopy. *Nuclear Instruments & Methods in Physics Research. Section B, Beam Interactions with Materials and Atoms*, *58*(1), 85–97. https://doi.org/10.1016/0168-583X(91)95681-3

Ravindra Babu, S., Nguyen, L. S. P., Sheu, G.-R., Griffith, S. M., Pani, S. K., Huang, H.-Y., & Lin, N.-H. (2022). Long-range transport of La Soufrière volcanic plume to the western North Pacific: Influence on atmospheric mercury and aerosol properties. *Atmospheric Environment*, *268*, 118806. https://doi.org/10.1016/j.atmosenv.2021.118806

Royer, H. M., Pöhlker, M. L., Krüger, O., Blades, E., Sealy, P., Lata, N. N., et al. (2023). African smoke particles act as cloud condensation nuclei in the wintertime tropical North Atlantic boundary layer over Barbados. *Atmospheric Chemistry and Physics*, *23*(2), 981–998. https://doi.org/10.5194/acp-23-981-2023

Sarmiento, J. L. (1993). Atmospheric CO_2 stalled. *Nature*, *365*(6448), 697–698. https://doi.org/10.1038/365697a0

Sarthou, G., Baker, A. R., Kramer, J., Laan, P., Laës, A., Ussher, S., et al. (2007). Influence of atmospheric inputs on the iron distribution in the subtropical North-East Atlantic Ocean. *Marine Chemistry*, *104*(3), 186–202. https://doi.org/10.1016/j.marchem.2006.11.004

Sedwick, P. N., Bowie, A. R., Church, T. M., Cullen, J. T., Johnson, R. J., Lohan, M. C., et al. (2020). Dissolved iron in the Bermuda region of the subtropical North Atlantic Ocean: Seasonal dynamics, mesoscale variability, and physicochemical speciation. *Marine Chemistry*, *219*, 103748. https://doi.org/10.1016/j.marchem.2019.103748

Shelley, R. U., Landing, W. M., Ussher, S. J., Planquette, H., & Sarthou, G. (2018). Regional trends in the fractional solubility of Fe and other metals from North Atlantic aerosols (GEOTRACES cruises GA01 and GA03) following a two-stage leach. *Biogeosciences*, *15*(8), 2271–2288. https://doi.org/10.5194/bg-15-2271-2018

Spirakis, C. S. (1991). Iron fertilization with volcanic ash? *Eos*, *72*(47), 525. https://doi.org/10.1029/90EO00370

Stewart, C., Damby, D. E., Tomašek, I., Horwell, C. J., Plumlee, G. S., Armienta, M. A., et al. (2020). Assessment of leachable elements in volcanic ashfall: A review and evaluation of a standardized protocol for ash hazard characterization. *Journal of Volcanology and Geothermal Research*, *392*, 106756. https://doi.org/10.1016/j.jvolgeores.2019.106756

Stewart, C., Horwell, C., Plumlee, G., Cronin, S., Delmelle, P., Baxter, P., et al. (2013). Protocol for analysis of volcanic ash samples for assessment of hazards from leachable elements. https://www.ivhhn.org/images/pdf/volcanic_ash_leachate_protocols.pdf

Tagliabue, A., Buck, K. N., Sofen, L. E., Twining, B. S., Aumont, O., Boyd, P. W., et al. (2023). Authigenic mineral phases as a driver of the upper-ocean iron cycle. *Nature (London)*, *620*(7972), 104–109. https://doi.org/10.1038/s41586-023-06210-5

Taylor, I. A., Grainger, R. G., Prata, A. T., Proud, S. R., Mather, T. A., & Pyle, D. M. (2023). A satellite chronology of plumes from the April 2021 eruption of La Soufrière, St Vincent. *Atmospheric Chemistry and Physics*, *23*(24), 15209–15234. https://doi.org/10.5194/acp-23-15209-2023

Vergara-Jara, M. J., Hopwood, M. J., Browning, T. J., Rapp, I., Torres, R., Reid, B., et al. (2021). A mosaic of phytoplankton responses across Patagonia, the southeast Pacific and the southwest Atlantic to ash deposition and trace metal release from the Calbuco volcanic eruption in 2015. *Ocean Science*, *17*(2), 561–578. https://doi.org/10.5194/os-17-561-2021

Wadsworth, F. B., Vasseur, J., Casas, A. S., Delmelle, P., Hess, K.-U., Ayris, P. M., & Dingwell, D. B. (2021). A model for the kinetics of high-temperature reactions between polydisperse volcanic ash and SO_2 gas. *American Mineralogist*, *106*(8), 1319–1332. https://doi.org/10.2138/am-2021-7691

Witham, C. S., Oppenheimer, C., & Horwell, C. J. (2005). Volcanic ash-leachates: A review and recommendations for sampling methods. *Journal of Volcanology and Geothermal Research*, *141*(3), 299–326. https://doi.org/10.1016/j.jvolgeores.2004.11.010

Yu, H., Chin, M., Bian, H., Yuan, T., Prospero, J. M., Omar, A. H., et al. (2015). Quantification of trans-Atlantic dust transport from seven-year (2007–2013) record of CALIPSO lidar measurements. *Remote Sensing of Environment*, *159*, 232–249. https://doi.org/10.1016/j.rse.2014.12.010

Zhang, R., Jiang Tao, J. T., Tian Yuan, T. Y., Xie Shucheng, X. S., Zhou Lian, Z. L., Li Qian, L. Q., & Jiao Nianzhi, J. N. (2017). Volcanic ash stimulates growth of marine autotrophic and heterotrophic microorganisms. *Geology*, *45*(8), 679–682. https://doi.org/10.1130/G38833.1

Zuidema, P., Alvarez, C., Kramer, S. J., Custals, L., Izaguirre, M., Sealy, P., et al. (2019). Is summer African dust arriving earlier to Barbados? The updated long-term in situ dust mass concentration time series from ragged point, Barbados, and Miami, Florida. *Bulletin of the American Meteorological Society*, *100*(10), 1981–1986. https://doi.org/10.1175/BAMS-D-18-0083.1

References From the Supporting Information

Barbeau, K., Moffett, J. W., Caron, D. A., Croot, P. L., & Erdner, D. L. (1996). Role of protozoan grazing in relieving iron limitation of phytoplankton. *Nature (London)*, *380*(6569), 61–64. https://doi.org/10.1038/380061a0

Bruland, K. W., & Rue, E. L. (2001). Analytical methods for the determination of concentration and speciation of iron. In D. R. Turner & K. A. Hunter (Eds.), *The biogeochemistry of iron in seawater* (pp. 256–284). John Wiley.

Mackey, K. R. M., Roberts, K., Lomas, M. W., Saito, M. A., Post, A. F., & Paytan, A. (2012). Enhanced solubility and ecological impact of atmospheric phosphorus deposition upon extended seawater exposure. *Environmental Science & Technology*, *46*(19), 10438–10446. https://doi.org/10.1021/es3007996

Prospero, J. M., Delany, A. C., Delany, A. C., & Carlson, T. N. (2021). The discovery of African dust transport to the Western hemisphere and the Saharan air layer: A history. *Bulletin of the American Meteorological Society*, *102*(6), E1239–E1260. https://doi.org/10.1175/BAMS-D-19-0309.1

Wells, M. L., Price, N. M., & Bruland, K. W. (1995). Iron chemistry in seawater and its relationship to phytoplankton: A workshop report. *Marine Chemistry*, *48*(2), 157–182. https://doi.org/10.1016/0304-4203(94)00055-I